Transcriptome dynamics predict thermotolerance in *Caenorhabditis elegans*

Katharina Jovic[1,#], Jacopo Grilli[2,3,5,#], Mark G. Sterken[1], Basten L. Snoek[1,4], Joost A. G. Riksen[1], Stefano Allesina[2,*], Jan E. Kammenga[1,*]

[1]Laboratory of Nematology, Wageningen University, Droevendaalsesteeg 1, 6708 PB, The Netherlands

[2]Department of Ecology and Evolution, University of Chicago, 1101 E 57th st., Chicago, IL, 60637, USA

[3]Santa Fe Institute, 1399 Hyde Park rd, Santa Fe, NM, 87501, USA

[4]Theoretical Biology and Bioinformatics, Utrecht University, Padualaan 8, 3584 CH, The Netherlands

[5]The Abdus Salam International Center for Theoretical Physics (ICTP), Strada Costiera 11, I-34014 Trieste, Italy

# These authors contributed equally to this work

* Corresponding authors

Keywords: Heat stress, Recovery, *C. elegans*, Resilience, Thermotolerance, Gene-expression dynamics, Transcriptome

Abstract

Background: The detrimental effects of a short bout of stress can persist, and potentially turn lethal, long after the return to normal conditions. Thermotolerance, which is the capacity of an organism to withstand relatively extreme temperatures, is influenced by the response during stress exposure, as well as the recovery process afterwards. While heat-shock response mechanisms have been studied intensively, predicting thermal tolerance remains a challenge.

Results: Here, we use the nematode *Caenorhabditis elegans* to measure transcriptional resilience to heat stress and predict thermotolerance. Using high dimensionality reduction techniques in combination with genome-wide gene expression profiles collected in three high resolution time-series during control, heat stress and recovery conditions, we infer a quantitative scale capturing the extent of stress-induced transcriptome dynamics in a single value. This scale provides a basis for evaluating transcriptome resilience, defined here as the ability to depart from stress-expression dynamics during recovery. Independent replication across multiple highly divergent genotypes reveals that the transcriptional resilience parameter measured after a spike in temperature is quantitatively linked to long-term survival after heat stress.

Conclusion: Our findings imply that thermotolerance is an intrinsic property that pre-determines long term outcome of stress and can be predicted by the transcriptional resilience parameter. Inferring the transcriptional resilience parameters of higher organisms could aid in evaluating rehabilitation strategies after stresses such as disease and trauma.

Background

Temperature is a key factor that directly affects physiological processes, life history and behaviour of many organisms. Ambient temperatures can rise suddenly, inflicting physiological consequences often lasting far beyond the initial exposure. For instance, it has repeatedly been shown that exposure to heat stress early in life can have an effect on traits later in life such as reproductive success and lifespan in the

44 nematode *Caenorhabditis elegans* and fruit fly *Drosophila melanogaster* [1–5]. The ability to withstand the
45 negative effects of heat stress is called thermotolerance and requires instant regulatory protective responses
46 involving the well-studied heat-shock response [6]. Since tolerance is a trait that results in the absence of
47 adverse effects, it is difficult to predict tolerance levels of an organism before the negative effects of stress
48 have become apparent.

49 Next to the induction of genes within specific stress-response pathways, recent studies in *C. elegans*
50 have shown that heat stress also induces a broad acclimation of transcriptional patterns involving differential
51 expression of thousands of genes [7–9]. Furthermore, during prolonged stress exposure, expression changed
52 continuously until lethal stress levels were reached [8]. Those findings illustrate that the state of the
53 transcriptome directly reflects the stress levels the organism was exposed to. While the reactive processes
54 occurring during the heat-shock response are well understood, much less is clear about how organisms
55 recover from a heat shock and how the genome wide transcriptional state might be used to predict long-term
56 outcome of a short bout of heat stress.

57 Here, we quantify gene expression resilience during and after heat stress in order to predict
58 thermotolerance in *C. elegans.* First, by measuring genome-wide gene expression levels of the canonical
59 laboratory strain Bristol N2 in three high-resolution time series (development, heat stress, and recovery from
60 heat stress), and applying high dimensionality reduction techniques to the data, we show that the state of the
61 transcriptome during and after the dynamic response to heat-stress perturbations can be captured by a single
62 parameter. This finding provides the basis to evaluate and compare complex transcriptional patterns after
63 stress in a straight forward and quantitative way.

64 Secondly, in order to generalize our findings beyond the individual genotype, we expanded our
65 analyses across different genetic backgrounds. Previous research shows that different genotypes are
66 differently affected by the heat stress [3, 9, 10], assumingly due to an intrinsic difference in thermal
67 tolerance. Our results show that transcriptome resilience measured after a mild heat stress early in the
68 development of *C. elegans* is predictive of its thermotolerance. Thermotolerance (based on long-term
69 survival) and transcriptional resilience were measured in independent populations of the same genotype,

70 emphasising the genetically intrinsic nature of thermal tolerance and the robustness of this approach to
71 predict thermal tolerance. Our methods are straightforward to implement and allow to map gene-expression
72 data during and after heat stress onto a few main quantitative scales that have a clear biological
73 interpretation.
74

75 # Results and discussion

76 **Using dimensionality-reduction techniques to infer a developmental axis *D* and heat-stress axis *H***

77 *C. elegans* develops relatively fast – within ~65 hours an individual develops from an egg into a
78 reproducing adult [11]. The transition through the four larval stages is controlled by highly dynamic
79 transcriptional processes [12, 13]. To characterize the temporal dynamics in genome-wide gene expression
80 during heat stress and in recovering *C. elegans* populations, we have to remove stress-independent variation
81 in gene-expression patterns caused by differences in development between samples collected in a time-
82 series spanning several hours. For this purpose, we compiled a data set of 71 gene expression profiles
83 measured in isogenic populations of the canonical strain Bristol (N2) sampled in an approximately hourly
84 interval during exposure to three different treatments: i) during unperturbed development at 20ºC [12], ii)
85 during prolonged exposure to heat-stress conditions at 35ºC [8], or iii) during a period of recovery at 20ºC
86 after a 2-hour heat stress at 35ºC (Fig. 1A). First, the data was separated into training and testing sets.
87 Second, through the application of dimensionality-reduction techniques (*i.e.* principal component analysis)
88 on expression profiles from unperturbed populations (n = 9 samples out of 18) and from heat-stressed
89 populations (n = 9 samples out of a total 39), we inferred the combination of gene-expression patterns that
90 best characterized the overall expression dynamics of each treatment (Fig. 1B, Methods, and SI). From the
91 unperturbed data, we obtained a *developmental axis D* (see SI section S2), describing the temporal
92 expression dynamics during development. Subsequently, the developmental influences captured by *D* were
93 removed from the data set of heat-stressed nematodes, allowing for the inference of the *heat-stress axis H*.
94 *H* describes temporal expression patterns induced by heat stress, while disregarding heat-stress-independent

temporal transcriptional patterns. Hence, by combining the data of perturbed and unperturbed populations, we were able to disentangle the effects of development and heat stress in time.

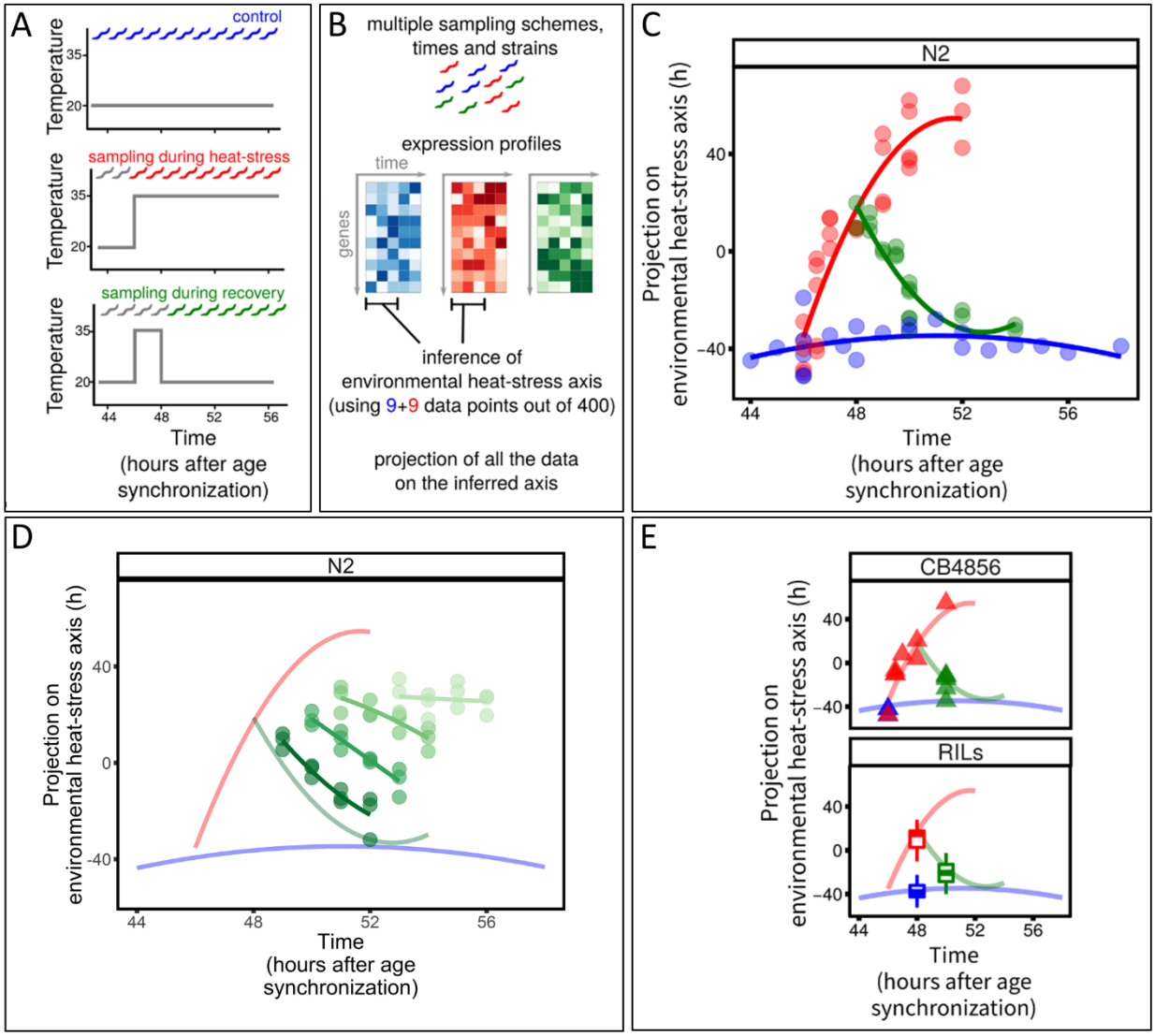

Figure 1. **Experimental setup and expression dynamics during heat-stress perturbations. A,** Experimental design of the three main treatments: control (blue; 20ºC throughout development), heat stress (red; populations shifted to 35ºC after 46 hours of development at 20ºC), and recovery (green; at 20ºC after heat stress). **B,** A subset of samples from heat-stress and control treatments were used for the inference of the heat-stress axis, *H*, describing the gene expression dynamics during heat stress. **C,** Projection of the data on this axis describes the dynamics of the response to heat stress. Notably, this is true also for the recovery data that was not used to infer axis *H*. **D,** Projection of transcriptome data of the recovery process after 2, 3,

105 4, and 6 hours of heat-stress shows a decrease in recovery dynamics. **E,** Axis *H* also describes the
106 transcriptional heat-stress response for strains other than N2.
107
108 **Heat-stress axis *H* reflects exposure duration, as well as recovery from heat stress**
109 By projecting gene-expression profiles on the heat-stress axis *H*, each sample can be associated with
110 a value *h.* While only 18 samples were used to infer the axis, all 71 samples from all three time-series align
111 along the axis according to treatment and exposure duration (Fig. 1C and Supplementary Figure S7),
112 showing that *h* is a quantitative measure of the transcriptional stress response. The value of *h* increased with
113 increasing heat-stress duration (Fig. 1C, red) until *h* started to saturate after long exposure (>4 hours). The
114 unperturbed worms had a constant value of *h* (Fig. 1C, blue), showing that we were able to successfully
115 remove the signal caused by developmental differences on gene expression. Strikingly, even though samples
116 collected during recovery were not used to determine the axis *H*, the gene expression during recovery from
117 a 2-hour heat stress was also well-explained with samples returning to the level of *h* typical of unperturbed
118 worms within about four hours (Fig. 1C, green). We concluded that *h* quantitatively reflects exposure
119 duration, as well as the time elapsed since the end of exposure. Note that although samples returned to the
120 pre-stress treatment level of *h* after recovery, this does not imply that recovered *C. elegans* populations are
121 transcriptionally indistinguishable from unperturbed ones (see SI section S2 and figure S7b). Therefore,
122 recovery was defined and measured here by the ability to depart from stress response dynamics.
123 So far, the results have shown that the transcriptional recovery process after a mild stress can be
124 followed over time using the heat-shock axis *H*. To exclude the possibility that *H* only captured time since
125 the end of the heat stress without biological meaning towards phenotypic recovery or resilience, we
126 expanded the dataset to include four additional time-series tracking the transcriptome recovery for 4 hours
127 following four different heat-stress intensities (2, 3, 4, and 6 hours at 35°C). The long-term effect of these
128 stress intensities on survival, reproduction, and mobility have been shown to range from mild after short (2
129 hour) exposure to 100% mortality within 24 hours after 6 hours at 35°C [8]. Fig. 1D shows that mildly
130 stressed population transcriptionally returned to pre-stress levels of *h* during the observed recovery period,

131 while increasing stress duration led to a slowing down of the transcriptional recovery process, and severely
132 stressed populations remained at a constant high value of *h.* Therefore, *H* can distinct between the progress
133 of the recovering transcriptome and a non-recovering transcriptome.
134
135 **Heat-stress axis *H* retains essential features of the biology of the heat-stress response**
136 Having shown that the axis *H* recapitulates the transcriptional state during and after exposure to
137 heat stress, we investigated the biological properties of the axis *H*. To this end, we performed an enrichment
138 analysis to determine which groups of genes contributed the most to the axis *H* (Fig. 2). Consistent with
139 expectations, genes encoding for stress response proteins (in particular heat-shock proteins *hsp*) and
140 nucleosomes (in particular histones *his*) were upregulated. These gene classes have previously been shown
141 to be highly activated by heat stress [7–9, 14]. Similarly, the value of *h* is negatively correlated with some
142 genes involved in cell metabolism such as ATPase transmembrane proteins. This analysis shows that the
143 axis *H* retains essential features of the biology of the heat-stress response, while summarizing these complex
144 biological dynamics into a single quantitative parameter.
145

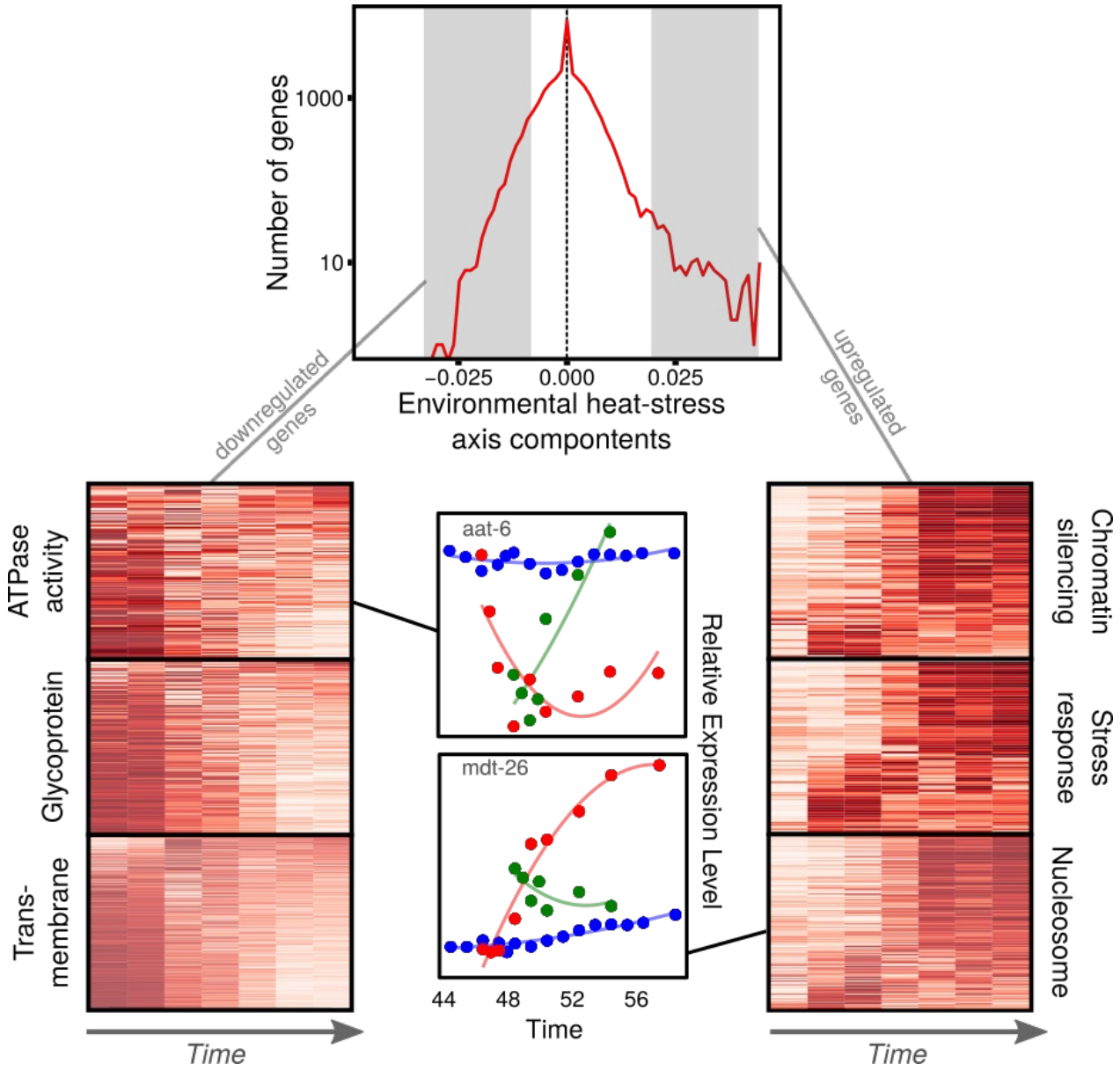

Figure 2. Single gene contribution to heat-stress axis, *H*. Distribution of the entries of the heat-stress axis (top of the figure). The distribution is not symmetric, which means that most genes (relatively to their unperturbed level of expression) are upregulated during heat-stress response. Enrichment results including two example of genes with negative and positive components (red corresponds to expression levels measured during heat stress, green corresponds to recovery, and blue to development).

154 **Heat-stress axis *H* reflects the average heat-stress response across multiple genotypes.**

155 Next, we tested whether heat-stress axis *H* can also reflect the change in gene expression for
156 different genotypes. We used expression profiles of the strain CB4856 (Hawaii), which is genetically
157 distinct from N2, as well as 54 recombinant inbred lines (RILs) [9], which are genetic mosaics derived from
158 a cross between CB4856 and N2 [15, 16]. We found that the heat-stress axis *H* successfully recapitulates
159 the average dynamic transcriptional response and resilience of this genetically diverse set of lines (Fig. 1E
160 and SI section S3). The robustness of the pattern across genotypes reflects the high degree of conservation
161 in transcriptional resilience. It should be noted that the RILs were not used here for the genetic mapping of
162 traits [17], but rather as a genotypic library.

163

164 **Variation in stress resilience across genotypes is captured in a genetic heat-stress axis (*GH*)**

165 We have shown that the heat-stress axis *H*, inferred using solely the isogenic strain N2, describes
166 the *average* conserved stress response of a library of highly divergent genotypes. On the other hand, there
167 is large natural variation in long-term effects of heat-stress exposure across genotypes, for example marked
168 by differences in the stressed transcriptome [9], survival rates [3, 18], and reproductive rates [3].
169 Considering that variation is genotype dependent, it implies a difference in transcriptional resilience during
170 and/or after stress. Next, we ask if a single axis could also capture the natural variation in heat-stress
171 response across genotypes. Since genotypes differ in more traits than their transcriptional response to stress,
172 such as developmental timing and size, we needed to isolate stress-induced variation in expression levels
173 from other intrinsic differences in the transcriptome between genotypes. For this purpose, we used gene
174 expression data of RILs collected before and after two hours of heat stress [9]. Analogous to our approach
175 above in inferring the heat-stress axis *H* for N2 by removing developmental differences, we corrected the
176 heat-stress response of the RILs for their intrinsic gene expression differences in unperturbed conditions
177 (see SI section S3). We inferred a *genetic heat-stress axis* (*GH*) that isolates and describes the variability
178 across strains in their stress response.

179 The strength of relationship between the genetic axis *GH* and the environmental heat-stress axis *H*
180 measures the proportion of the variation of heat-stress response across RILs that is due to timing differences.
181 We found a positive correlation between the two axes (Spearman rho = 0.36, p = 0.01) implying that
182 different strains respond as if they were exposed to the heat stress for different durations. This was confirmed
183 by analysing a second set of heat-stressed gene expression profiles from a separate alternative panel of
184 inbred lines [19, 20](Introgression Lines, ILs; Spearman rho = 0.44, $p = 8 \cdot 10^{-4}$) (Fig. 3). These results show
185 that the genetic differences also lead to difference in the timing or magnitude of the transcriptional response.
186 The presence of a correlation between the axes *H* and *GH* also implies that the value of *gh* (the projection
187 of the gene expression profile on the axis *GH*) recapitulates the relative strength of the heat-stress response:
188 the higher the value of *gh*, the farther away is the gene expression profile from the unperturbed state or, in
189 other words, the lower its transcriptional resilience to heat-stress.
190

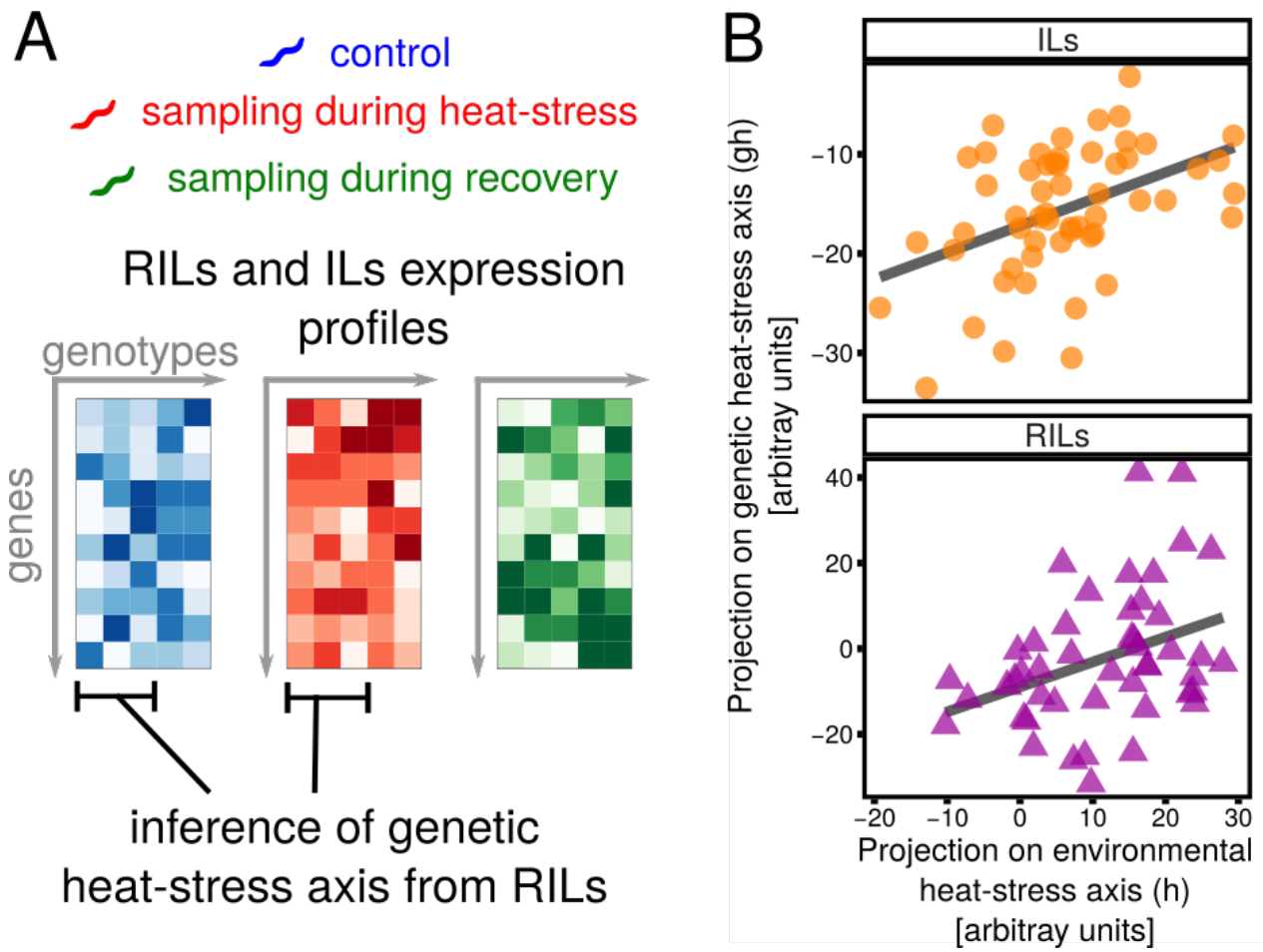

Figure 3. Derivation of the genetic heat-stress axis, *GH*, and relation with environmental heat-stress axis, *H*. A, For each RIL and IL, we measured gene expression in absence of perturbation, after two hours exposure to heat stress and during recovery (after two hours of the end of a two-hour heat stress). Using only RIL data, we obtain the genetic heat-stress axis (*GH*), describing the difference between RILs in heat-stress response (discounting their differences in gene expression in the unperturbed case). **B,** Correlation between genetic heat-stress axis and the environmental heat-stress axis shown for heat-stress samples of RILs and ILs.

202 **Transcriptional resilience on a short timescale is predictive of the variability in thermotolerance on a**
203 **longer timescale**

204 Heat stress affects gene expression dynamics and resilience in the short term in a predictable way, which is
205 recapitulated by axes *H* and *GH*. On the other hand, in the long run, heat stress also affects developmental
206 speed, aging, behaviour, and vitality - for instance by drastically reducing lifespan. We set out to explore
207 how the variability in gene expression dynamics following heat stress on a short timescale is predictive of
208 variability in thermotolerance measured on a longer timescale. Thermotolerance in *C. elegans* can be
209 recorded by its survival rates. Therefore, in a parallel experiment, we collected lifespan data of over 200
210 different RILs and ILs with and without exposure to heat stress. While two hours at 35°C are sufficient to
211 induce a strong transcriptional response, previous experiments have shown that overall lifespan is not
212 necessarily shortened at this intensity [8]. Therefore, we increased the exposure duration to four hours at
213 35°C for lifespan measurements as this duration is known to affect lifespan [3, 8], allowing us to make a
214 better estimate of difference in thermotolerance across genotypes As expected, both RILs and ILs show high
215 variability in their lifespan after heat stress and in control conditions. The average lifespan following a heat
216 stress is always lower than what was found for the same strain when unperturbed (Fig. 4 and Figure S14).

217 Next, we compared the effect of heat stress on the lifespan of different RILs with the difference in
218 transcriptional resilience, measured by projecting the recovery data of the RILs on the genetic heat-stress
219 axis *GH*. Figure 4 shows that the ability of different strains to recover from heat stress is predictive of
220 thermotolerance (Spearman rho = -0.41, p = 0.02; Fig 4). In order to test the robustness of this result, we
221 also performed the same analysis on ILs, which are genetically mostly derived from one strain (N2) and
222 were not used to infer the axis. In this case, we also found a significant correlation (Spearman rho = -0.46,
223 $p = 10^{-3}$), implying that the connection between the ability to recover and lifespan was robust across different
224 inbred line panels. The projection of the heat-stress data onto *GH* (which is related to the speed at which
225 worms react to heat stress) was not robustly correlated with lifespan (see SI section S5), showing that
226 resilience measured based on recovery data was more directly linked to tolerance.

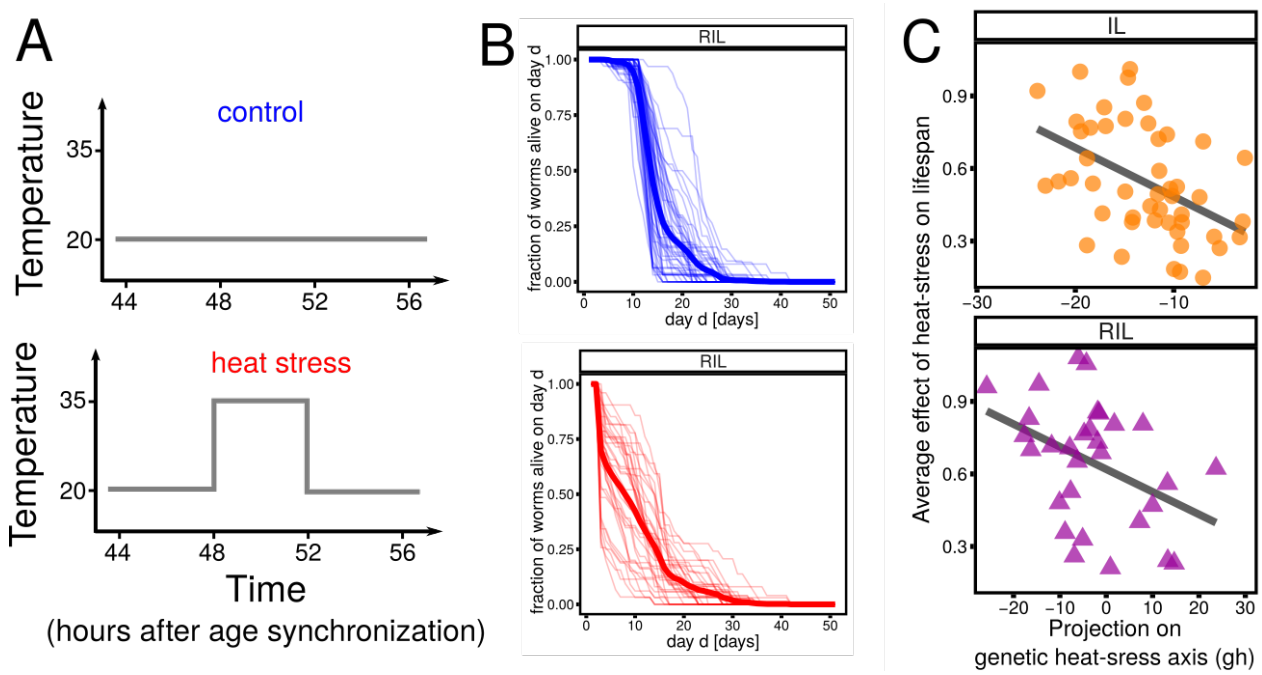

Figure 4. Effect of heat stress on lifespan and correlation with gene expression recovery. **A,** Experimental set-up used to collect lifespan data of 40 RILs and 54 ILs. **B,** Comparison of the cumulative lifespan distribution of unperturbed (blue) and perturbed (red) RILs. Each thin line corresponds to a RIL (an average of 31 animals were scored per genotype and treatment), while the thick line is the average across RILs. **C,** Effect of heat stress on lifespan (measured as the ratio of the average lifespan after perturbation and without perturbation) correlates with the projection of recovery data on the genetic heat-stress axis for RILs and ILs. Strains recovering faster from heat stress experience a weaker effect on their lifespan.

Conclusions

This study sheds light on how organisms recover from environmental stress perturbations, by means of a systemic *modus operandi* based on using genome-wide gene expression profiles. We conclude that a relatively simple axis can measure stress resilience of a dynamic transcriptome in a single quantitative variable and describes the capacity of an organism to recover from heat stress. Our findings show that natural variation in transcriptome resilience after mild stress exposure is predictive of thermotolerance across a

242 diverse set of genotypes in *C. elegans*. The results imply that thermotolerance is an intrinsic trait that largely
243 pre-determines long-term effects of heat-stress exposure. Operationalizing the concept of resilience in
244 higher organisms, like mammals, has been difficult because it includes a range of many different phenotypic
245 traits [21]. Our approach represents a novel way in understanding resilience in a living system, and we show
246 how the inherent complexity of stress recovery can be exploited to predict the chance of survival. We
247 anticipate that our finding will accelerate progress in the study of resilience of complex living systems,
248 opening up new avenues of research in stress, aging, and disease across other species.
249

250 # Methods

251 **Strains and Maintenance**

252 The wild-type *C. elegans* strains N2 (Bristol) and CB4856 (Hawaii) were used in this study, as well as 54
253 CB4856 x N2 recombinant inbred lines (RILs; each line is a genetic mosaic with contributions of the two
254 parental strains [9, 15, 16], and 47 CB4856 x N2 introgression lines (ILs; one individual locus of the CB4856
255 genome introgressed into an otherwise N2 genetic background [19]). Strains were maintained under
256 standard culturing conditions on (9 cm diameter) Petri dishes with Nematode Growth Medium (NGM)
257 containing *Escherichia coli* OP50 as food source [22]. To prepare populations for the start of an experiment,
258 maintenance populations were chunked to fresh 9-cm NGM plates with food and kept at 20°C for exactly
259 one week to induce starvation. This was done to assure that all populations received the same treatment
260 before the experiment.
261

262 **Lifespan under heat stress and control conditions**

263 Starved populations were transferred to fresh NGM dishes seeded with *E. coli* OP50 by chunking, and grown
264 at 16°C or 20°C (depending on the desired growth rate) for 3-4 days to obtain proliferating populations. The
265 populations were age synchronized by hypochlorite treatment according to standard protocols [22] and

266 grown at 20°C until the 4th larval stage was reached. At 47 hours post age-synchronization, the larvae were
267 collected from the plates with M9 buffer, and 30-40 individuals were transferred to new NGM dishes
268 containing 5-fluorodeoxyuridine [23]. At 48 hours post age-synchronization, the heat-stress treated group
269 was exposed to 35°C for 4 hours. Control and post-heat-stress conditions were set to 20°C. Survival was
270 scored every day by checking the response to touch with a picking needle. For each genotype, an average
271 number of 31 animals were scored for each treatment.

272 For each genotype and treatment the survival curves are reported in Figure 4B. For each genotype
273 and treatment, we computed the average lifespan. The average effect of heat stress on lifespan (reported in
274 Fig. 4C) is the ratio between the average lifespan after heat stress and the average lifespan in the control.

275

276 **Transcriptome profile of heat stress, recovery and developmental state**

277 ***Data retrieval***

278 Sub-sets of the transcriptomic profiles used in this study have previously been described. These sub-sets
279 include the developmental time series previously described in Snoek *et al.* (2014) [12], retrieved from Array
280 Express https://www.ebi.ac.uk/arrayexpress/ under accession number E-MTAB-7019, which includes 22
281 transcription profiles of N2 populations sampled in hourly intervals between 44-58 hours post
282 synchronization. The heat-stress time series was described in Jovic *et al.* (2017) [8], which includes 29
283 transcription profiles established after an exposure to 35°C for 0, 0.5, 1, 2, 3, 4, 6, 8, or 12 hours starting at
284 46 hours after age-synchronization (retrieved from ArrayExpress under accession number E-MTAB-5753).
285 Transcription profiles of the RILs and ILs including the parental lines (N2 and CB4856) in control
286 conditions (sampled 48 hours post age-synchronization), after a 2-hour heat stress starting at 46 hours post
287 age-synchronization, and after a subsequent 2-hours recovery period were first presented by Snoek *et al.*
288 ([9]; data retrieved from ArrayExpress, accession number E-MTAB-5779) and Sterken *et al.*, ([20];
289 ArrayExpress, accession number E-MTAB-7424), respectively. A detailed overview of data sets and the
290 according publications can be found in Supplementary table 1.

291

292 ***Stress treatment and sampling for transcriptome analysis***

293 The above described transcriptome data-set was extended with a heat-stress time series for CB4856, and a
294 recovery time series for N2 using protocols adapted from Snoek *et al.* (2014, 2017) [9, 12] and Jovic *et al.*
295 (2017) [8]. Starved populations were transferred onto fresh NGM dishes seeded with *E. coli* OP50 by
296 chunking and grown at 16°C or 20°C for 3-4 days depending on the desired growth rate to obtain gravid
297 hermaphrodites. Age-synchronized populations were obtained by hypochlorite treatment according to
298 standard protocols [22] and maintained at 20°C until the begin of the heat-stress exposure of 35°C starting
299 at 46 hours post age synchronization. For the CB4856 heat-stress time series, samples were taken after 0,
300 0.5, 1, 2, 4, and 6 hours at 35°C by rinsing the populations of the NGM plates with M9 buffer. For the N2
301 recovery time series, samples were transferred to 20°C after 2, 3, 4, or 6 hours at 35°C. After 2 hours of
302 heat-stress, samples were taken 0, 0.5, 1, 1.5, 2, 4, and 6 hours into the recovery period; For 3, 4, or 6 hours
303 of heat stress, samples were taken in an hourly interval up to 4 hours post-exposure. All samples were
304 immediately flash frozen in liquid nitrogen at the time of collection, and stored at -80°C until further use.

305 ***RNA isolation***

306 mRNA was isolated from frozen samples using the Maxwell® 16 AS2000 instrument with a Maxwell® 16
307 LEV simplyRNA Tissue Kit (both Promega Corporation, Madison, WI, USA). The mRNA was isolated
308 according to protocol with a modified lysis step as described in Snoek *et al.* 2014, and Jovic *et al.* 2017. 200
309 µl homogenization buffer, 200 µl lysis buffer and 10 µl of a 20 mg/ml stock solution of proteinase K were
310 added to each sample. The samples were then incubated for 10 minutes at 65°C and 1000 rpm in a
311 Thermomixer (Eppendorf, Hamburg, Germany) before cooling on ice for 1 minute. At this point, the
312 samples were pipetted into the cartridges resuming with the standard protocol.

313 ***Sample preparation and scanning***

314 For cDNA synthesis, labelling and the hybridization reaction, the 'Two-Color Microarray-Based Gene
315 Expression Analysis; Low Input Quick Amp Labeling' - protocol, version 6.0 from Agilent (Agilent
316 Technologies, Santa Clara, CA, USA) was followed, starting at step 5. The Agilent *C. elegans* (V2) Gene
317 Expression Microarray 4X44K slides were used in combination with an Agilent High Resolution C Scanner
318 using the recommended settings. Data was extracted with the Agilent Feature Extraction Software (version
319 10.7.1.1) following the manufacturers' guidelines.

320 ***Data normalization***

321 Microarray data were normalized using a within array normalization using a standard function of the R
322 package limma (using "loess" method) [24].
323 The code needed to replicate all the results presented here can be found at
324 https://github.com/jacopogrilli/resiliencevitality.git

325 Availability of data and materials

326 Newly produced raw and processed transcriptome datasets supporting the conclusions of this article are
327 available in the ArrayExpress database at EMBL-EBI (www.ebi.ac.uk/arrayexpress; [25]) under the
328 accession number E-MTAB-7007 and E-MTAB-7948.

329 Acknowledgements

330 We thank Miriam Rodriguez, Roel P. J. Bevers, Rita Volkers, Rosanne Bartels, Yvonne Laven for the
331 assistance with collecting data. This research was financed by the Human Frontiers Science Program (grant
332 RGP0028-2014). We thank Ben Lehner, Riekelt Houtkooper, Marco Cosentino Lagomarsino, Zachary
333 Miller, and Wim van der Putten for helpful discussions about the manuscript.

334 Author Contributions

335 KJ, JG, SA and JEK wrote the manuscript. MGS and BLS commented on the manuscript. KJ, MGS and
336 JAGR performed and supervised the experiments. KJ, MGS and BLS assembled, annotated and curated the
337 microarray data. JG performed the analysis and wrote the code.

338 Disclosure Declarations

339 Authors do not have competing interests.

340 References

341 1. Le Bourg E, Valenti P, Lucchetta P, Payre F. Effects of mild heat shocks at young age on aging and
342 longevity in Drosophila melanogaster. Biogerontology. 2001;2:155–64. doi:10.1023/A:1011561107055.

343 2. Lithgow GJ, White TM, Melov S, Johnson TE. Thermotolerance and extended life-span conferred by
344 single-gene mutations and induced by thermal stress. Proc Natl Acad Sci U S A. 1995;92:7540–4.
345 doi:10.1073/pnas.92.16.7540.

346 3. Rodriguez M, Snoek LB, Riksen JAG, Bevers RP, Kammenga JE. Genetic variation for stress-response
347 hormesis in C. elegans lifespan. Exp Gerontol. 2012;47:581–7. doi:10.1016/j.exger.2012.05.005.

348 4. Gouvêa DY, Aprison EZ, Ruvinsky I. Experience modulates the reproductive response to heat stress in
349 C. elegans via multiple physiological processes. PLoS One. 2015;10:1–27.

350 5. Snoek BL, Volkers RJM, Nijveen H, Petersen C, Dirksen P, Sterken MG, et al. A multi-parent
351 recombinant inbred line population of C. Elegans allows identification of novel QTLs for complex life
352 history traits. BMC Biol. 2019;17:24. doi:10.1186/s12915-019-0642-8.

353 6. Morimoto RI. Regulation of the heat shock transcriptional response: Cross talk between a family of heat
354 shock factors, molecular chaperones, and negative regulators. Genes Dev. 1998;12:3788–96.
355 doi:10.1101/gad.12.24.3788.

356 7. Brunquell J, Morris S, Lu Y, Cheng F, Westerheide SD. The genome-wide role of HSF-1 in the regulation
357 of gene expression in Caenorhabditis elegans. BMC Genomics. 2016;17:559. doi:10.1186/s12864-016-
358 2837-5.

359 8. Jovic K, Sterken MG, Grilli J, Bevers RPJJ, Rodriguez M, Riksen JAGG, et al. Temporal dynamics of
360 gene expression in heat-stressed Caenorhabditis elegans. PLoS One. 2017;12:e0189445.
361 doi:10.1371/journal.pone.0189445.

362 9. Snoek BL, Sterken MG, Bevers RPJ, Volkers RJM, Van't Hof A, Brenchley R, et al. Contribution of
363 trans regulatory eQTL to cryptic genetic variation in C. elegans. BMC Genomics. 2017;18:500.
364 doi:10.1186/s12864-017-3899-8.

365 10. Grishkevich V, Ben-Elazar S, Hashimshony T, Schott DH, Hunter CP, Yanai I. A genomic bias for
366 genotype-environment interactions in C. elegans. Mol Syst Biol. 2012;8:587. doi:10.1038/msb.2012.19.

367 11. Byerly L, Cassada RC, Russell RL. The life cycle of the nematode Caenorhabditis elegans. I. Wild-type
368 growth and reproduction. Dev Biol. 1976;51:23–33. doi:10.1016/0012-1606(76)90119-6.

369 12. Snoek LB, Sterken MG, Volkers RJM, Klatter M, Bosman KJ, Bevers RPJ, et al. A rapid and massive
370 gene expression shift marking adolescent transition in C. Elegans. Sci Rep. 2014;4:3912.
371 doi:10.1038/srep03912.

372 13. Francesconi M, Lehner B. The effects of genetic variation on gene expression dynamics during
373 development. Nature. 2014;505:208–11. doi:10.1038/nature12772.

374 14. Delaney K, Mailler J, Wenda JM, Gabus C, Steiner FA. Differential Expression of Histone H3.3 Genes
375 and Their Role in Modulating Temperature Stress Response in Caenorhabditis elegans. Genetics.
376 2018;209:551–65. doi:10.1534/genetics.118.300909.

377 15. Li Y, Álvarez OA, Gutteling EW, Tijsterman M, Fu J, Riksen JAG, et al. Mapping determinants of gene

378 expression plasticity by genetical genomics in C. elegans. PLoS Genet. 2006;2:2155–61.

379 16. Thompson OA, Snoek LB, Nijveen H, Sterken MG, Volkers RJM, Brenchley R, et al. Remarkably
380 divergent regions punctuate the genome assembly of the Caenorhabditis elegans hawaiian strain CB4856.
381 Genetics. 2015;200:975–89. doi:10.1534/genetics.115.175950.

382 17. Rockman M V., Kruglyak L. Genetics of global gene expression. Nat Rev Genet. 2006;7:862–72.
383 doi:10.1038/nrg1964.

384 18. Lucanic M, Plummer WT, Chen E, Harke J, Foulger AC, Onken B, et al. Impact of genetic background
385 and experimental reproducibility on identifying chemical compounds with robust longevity effects. Nat
386 Commun. 2017;8:14256. doi:10.1038/ncomms14256.

387 19. Doroszuk A, Snoek LB, Fradin E, Riksen J, Kammenga J. A genome-wide library of CB4856/N2
388 introgression lines of CB4856/N2 introgression lines of Caenorhabditis elegans. Nucleic Acids Res.
389 2009;37.

390 20. Sterken MG, Bevers RPJ, Volkers RJM, Riksen JAG, Kammenga JE, Snoek LB. Dissecting the eQTL
391 micro-architecture in Caenorhabditis elegans. bioRxiv. 2019;:651885. doi:10.1101/651885.

392 21. Russo SJ, Murrough JW, Han M-H, Charney DS, Nestler EJ. Neurobiology of resilience. Nat Neurosci.
393 2012;15:1475–84. doi:10.1038/nn.3234.

394 22. Brenner S. The genetics of Caenorhabditis elegans. Genetics. 1974;77:71–94.
395 doi:10.1002/cbic.200300625.

396 23. Hosono R. Sterilization and growth inhibition of Caenorhabditis elegans by 5-fluorodeoxyuridine. Exp
397 Gerontol. 1978;13:369–73. doi:10.1016/0531-5565(78)90047-5.

398 24. Ritchie ME, Phipson B, Wu D, Hu Y, Law CW, Shi W, et al. limma powers differential expression
399 analyses for RNA-sequencing and microarray studies. Nucleic Acids Res. 2015;43:e47.

400 doi:10.1093/nar/gkv007.

401 25. Athar A, Füllgrabe A, George N, Iqbal H, Huerta L, Ali A, et al. ArrayExpress update - from bulk to
402 single-cell expression data. Nucleic Acids Res. 2019;47:D711–5. doi:10.1093/nar/gky964.

403